

Dynamic processing of $\text{SiH}_4 + \text{CH}_4$ plasma induced by an infrared laser

G. S. Fu, W. Yu, X. W. Li, L. Han, and L. S. Zhang

Department of Physics, Hebei University, Baoding, 071002, People's Republic of China

(Received 6 February 1995)

In this paper, the time- and space-resolved optical emission spectrum is used to study dynamic processes in a $\text{SiH}_4 + \text{CH}_4$ plasma induced by a pulsed transversely excited atmosphere CO_2 laser. The main results include the following: (1) Based on the emission analysis of the plasma in different positions and experimental conditions, it is found that laser-induced breakdown of sample gases produced a detonation wave and then expanded in a similar manner to produce a shock wave. (2) Through the measurement of the time resolution of the profile of H_β emission, we found the deionization of the plasma is mainly due to the recombination of ions and electrons. (3) The time characteristics of the emission spectra of various fragments support the explanation that production of Si and C atoms are the main dissociation channels for SiH_4 and CH_4 in the plasma.

PACS number(s): 52.50.Jm, 82.40.-g, 47.40.-x

I. INTRODUCTION

The plasma induced by the interaction of a pulsed laser with gases, which possesses the characteristics of instantaneous heating and fast quenching, is widely used in studies of chemical analysis and high-temperature chemical reaction. In recent decades, the technique has been successfully applied in the fields of material manufacture, treatment, and synthesis. Using the method of transversely excited atmosphere (TEA) CO_2 laser-induced plasma chemical vapor deposition (LPCVD), we have successfully realized low-temperature deposition of large area silicon films having various crystal structures [1]. As a film-making technique, LPCVD overcomes the shortcomings of other CVD processing; for example, the low deposition rate and self-doping from the high-temperature substrate. Therefore, LPCVD provides another way to manufacture semiconductor materials. Experiments have shown that the technique also has good prospects for application in the synthesis of nanometer ceramic powder. It has been reported that superfine powders of SiC and Si_3N_4 have been synthesized by using a laser-induced plasma in the gas phase [2,3]. A laser-induced plasma includes complex physical-chemical processes, such as the excitation and dissociation of reacting molecules, the collision and reaction of various dissociated pieces, etc. [3]. Hence, to efficiently control the plasma and improve the characteristics of the resulting materials, it is necessary to clearly understand the processes in the plasma, its energy transport, the occurrence of molecular fragments in the plasma, and the dynamic mechanism of this processes.

Up to now, there have been many reports about the characteristics of a CH_4 or SiH_4 laser-induced plasma and the analysis of its reaction process [4–6]. However, the study of the reacting process of the plasma in mixed gaseous substances is still preliminary [3,4]. In the present work, a powerful TEA CO_2 laser is used to radiate a $\text{SiH}_4 + \text{CH}_4$ system for the production of the plasma. The time- and space-resolved optical emission spec-

trum is used to measure the plasma spectrum, the expansion process of the plasma wave, and the line broadening of H_β emission in the plasma. Based on the measured results, the gas breakdown process, the change of the plasma parameter, and the processing of macrodynamics have been carefully studied, and the dissociation mechanism of the reacting molecules and the reaction processes among the dissociated molecular fragments in the laser induced plasma are discussed.

II. EXPERIMENT

The experimental configuration used in this work is shown in Fig. 1. A sample cell is made from nylon with six optical windows, sealed by NaCl and quartz plates. The TEA CO_2 laser is operated at 10P(20), and the output energy of the laser pulse is variable from 0.2 to 1.4 J. The duration [the full width at half maximum (FWHM) of the main peak] of the laser pulse is 100 ns, with a low-intensity tail of 2 μs . A 2-Hz repetition rate of the laser pulse is used in this experiment. The laser beam is focused in the center of the cell with a 10-cm focal length NaCl lens. The radius of the laser beam at the focal point is 0.1 cm. After the breakdown of the sample gases, the luminescence of the plasma transmitting through the four side windows is detected by a photomultiplier (GDB-33), the end section of an optical fiber with a radius of 0.1 mm, a monochromator (Spex 1404), and an optical multichannel analyzer system (OMA III EG&G). The time characteristics of the luminescence in different regions of the plasma is measured by the optical fiber photomultiplier combination. The signal received is sent to channel 2 of the oscilloscope (Tektronix 7844). In order to guarantee sufficient resolution, an optical receiver is installed in front of the incident end of the optical fiber; therefore the spatial resolution is better than 0.07 mm. The OMA III is used to measure and analyze the time-integrated spectrum of the plasma. To measure the characteristics of the spectrum of various fragments in a single pulse, the monochromator is used to select the

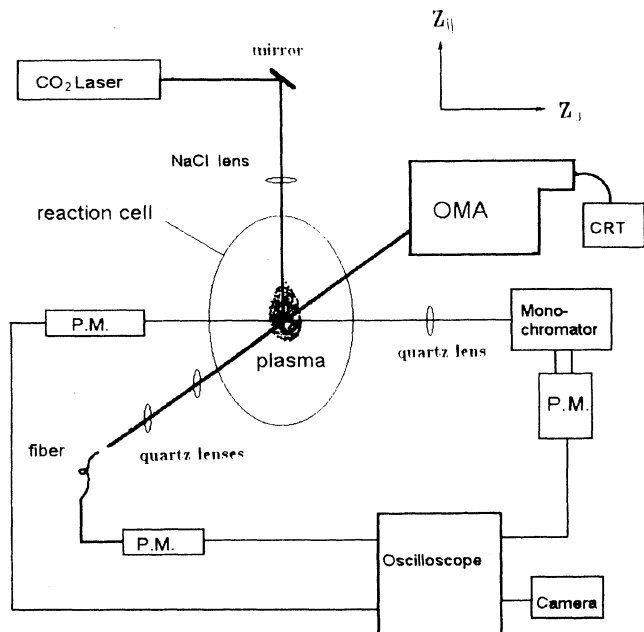


FIG. 1. Schematic diagram of the experimental apparatus.

characteristic spectrum of the different fragments, and the signal is displayed on the oscilloscope. The synchronous output of the laser is sent to the trigger of OMA III and oscilloscope. The sample in the cell is the mixture of $\text{SiH}_4 + \text{CH}_4 + \text{Ar}$ or $\text{SiH}_4 + \text{CH}_4 + \text{H}_2$ (the SiH_4 volume is 2.3%; that of CH_4 is 9.2%). The vacuum of the cell is about 10^{-2} torr.

III. RESULTS

A. Measurement of the time-resolved OES

The interaction between a focused CO_2 laser beam and mixed gases of $\text{SiH}_4 + \text{CH}_4 + \text{H}_2$ makes the gases break down, while SiH_4 and CH_4 molecules are dissociated. The plasma luminescence includes continuum radiation as a background, and the characteristic line emission of dissociated fragments. In order to understand the production and reaction of these dissociated fragments in the plasma and find the mechanism of the dissociation, the spectrum of the plasma radiation is measured. Figure 2 shows part of the time-integrated spectrum. Using well known assignments, the principal emitting substances measured by means of optical emission spectrum (OES) are the following:

Si: 250.4, 251.4, 251.6, 252.8, 263.0, 288.1, 390.6 (nm) ,
 C: 247.8, 909.4 (nm) , H: 656.3, 486.1, 434.0 (nm) ,
 Si^+ : 506.1, 634.7, 637.5 (nm) , Si_2 : 385.3, 393.3, 397.9 (nm) ,
 C^+ : 283.6, 426.7 (nm) , Si^{2+} : 254.3, 359.0, 455.2, 456.7 (nm) ,
 SiH : 410.4, 411.7, 412.8, 413.0 (nm) , SiH^+ : 399.6 nm , CH: 387.9 nm .

Figure 3 is the time-resolved OES spectrum. It shows that the profile of OES varies with time, and especially for different fragments the variations are different. This means that different fragments have different time characteristics.

Clearly understanding the change in the density of various dissociated fragments after the breakdown is important to determine the dissociation channel of the molecules in the laser-induced plasma. Therefore, some of the main emitting fragments are selected and measured in

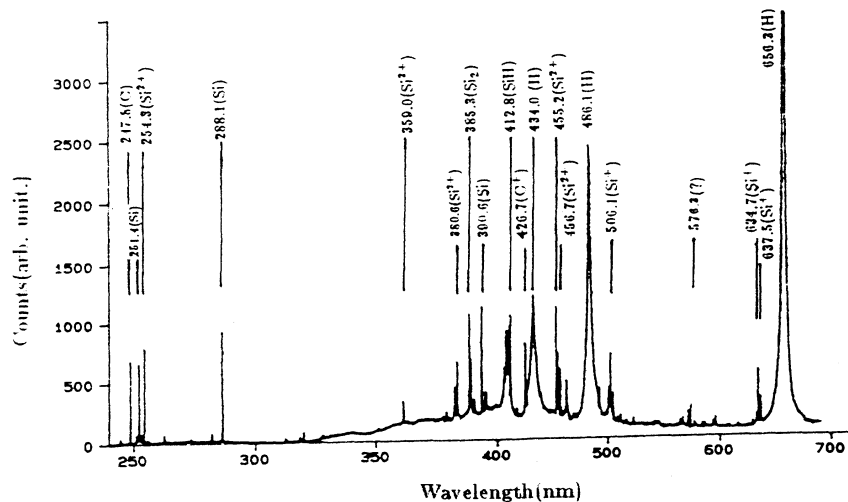


FIG. 2. The integrated optical emission spectrum.

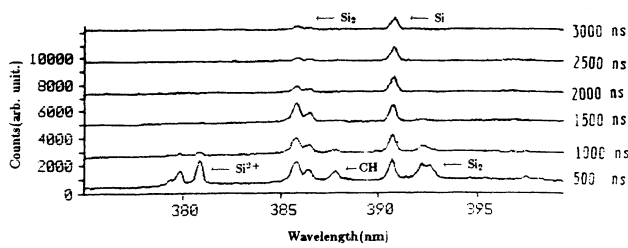


FIG. 3. Temporal change of the optical emission spectrum.

a single pulse by means of the photomultiplier-oscilloscope combination. In Fig. 4, the temporal shapes of the signal of the Si, C, and Si₂ fragments and emission at 625.0 nm are shown. Table I gives the position of the peak originating from the time of breakdown, the fast rise time, the relative amplitude, and the duration of the signal, respectively. It is obvious that the emissions of H, Si, C, and Si⁺ mainly initiate within 100 ns of the time of breakdown, while those of Si₂, SiH, C⁺, C²⁺, and Si²⁺ appear 200 ns after the breakdown.

B. Measurement of the average temperature of electron and the line profile of H_β emission

To find the reaction processes occurring in the plasma, the average electron temperature of the colliding electrons, which are the main exciting source of the plasma, is further studied, and the spectral broadening of H_α, H_β, and H_γ emission in the Balmer series is carefully measured. The result shows that the spectral width (FWHM) of the three lines increases with the principal quantum number of the upper state. At 100 ns, the ratio of integrated intensity of H_α to that of H_β emission is 2.63:1, which corresponds to an electron temperature is 3.6 eV [7]. The time characteristic of the H_β emitting result

TABLE I. Time characteristics of the main emitting fragments.

Fragments (nm)	Fast rise time (ns)	Peak time (ns)	Ratio ^a	Duration (μs)
C 247.8	50	600	1.2/1	13
Si 288.1	50	200	1.2/1	8.5
390.6	50	200	1.1/1	11
H 656.3	50	600	1.5/1	10
486.1	50	200	1.2/1	6.5
Si ⁺ 634.7	50	200	1.3/1	4
Si ²⁺ 455.2	50	300	2.6/1	2.5
SiH 412.8	50	300	2/1	4
Si ₂ 385.3	100	300	1.5/1	4.5
C ⁺ 426.7	50	300	3.5/1	2.7
C ²⁺ 229.7	100	400	1.5/1	2.5
625.0 ^b	50			3

^aAmplitude ratio of the peak signal and the fast rise section.

^bUnidentified emission.

shows that the spectral width of H_β emission is much wider in the initial time of the breakdown (its maximum width is more than 15 nm), and narrower with increasing time. Figure 5 shows the result of the time resolution measurement of H_β emission with 0.5 to 1.4 μs after the breakdown. From this figure, we see that the intensity and the central dip of the spectrum decrease with the time increase.

C. Space resolution measurement of the plasma radiation

To examine the dynamic processes from the plasma occurring in the material synthesis, the optic fiber photomultiplier system is used to observe the total radiation of the SiH₄ + CH₄ + Ar plasma in different positions. Figure 6 shows the time characteristic of the plasma radiation in Z_{||} = 2.6 mm (Z_{||} is the position away from the focal

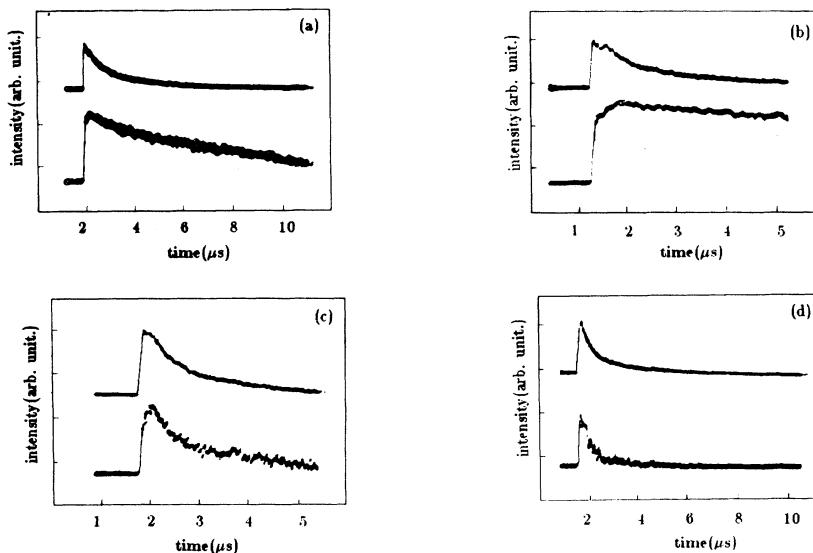


FIG. 4. Temporal shape of some fragments. Top line in each plot: total emission signal. Bottom line: (a) Si (390.6 nm), (b) C (247.8 nm), (c) Si₂ (385.3 nm), and (d) background 625.0 nm.

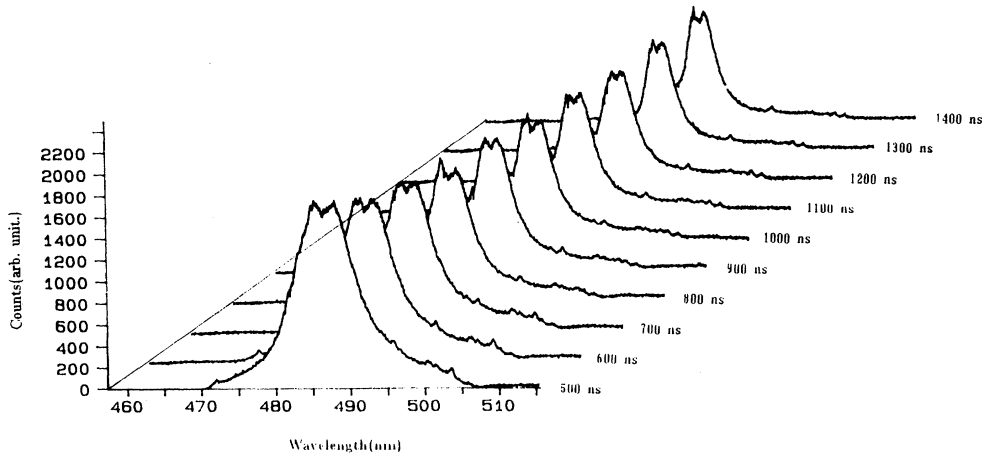


FIG. 5. The line profiles of $\text{H}\beta$ emission at different times.

point opposite to the direction of incident laser beam; see Fig. 1).

The profile of the signal gives the change of the density of the excited gas particles in the observed area. The signal in the time range of $t_o - t_l$ is from the emission of plasma which is directly produced by the laser. Because of the lower intensity of the laser away from the focus point, the signal in this range of time is relatively weak. From the time shape at $Z_{\parallel} = 2.6$ mm, we see that the peak position of luminescence is at $t_l = 390$ ns after t_o (the beginning luminescence time). Notice that the interaction between laser and gases mainly occurs within 200 ns (i.e., within the main peak duration of the laser pulse), so that the stronger emission occurring in t_l shows that the strong breakdown in the focus area brings out a shock wave, which propagates to the position Z_{\parallel} after 390 ns and causes the emission of the particles in the observed area. The signal measured at different positions shows that with the increase of the distance Z_{\parallel} from the focus point, the signal shows an obvious jump at t_l and the time delay with the increase of Z_{\parallel} . Figure 7 shows the relation of t_l and the observed position Z_{\parallel} in the opposite direction, position Z_{\perp} in the vertical direction of the incident laser beam. From this result, we see that, in the

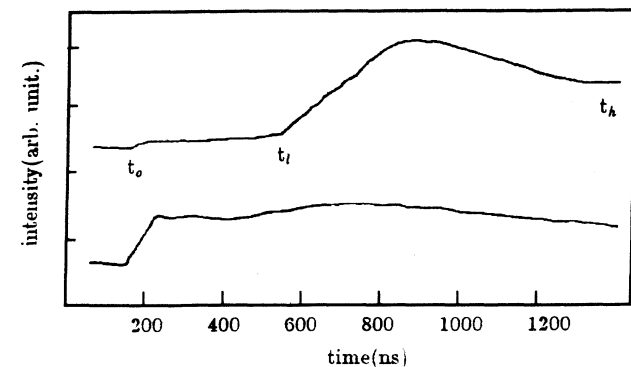


FIG. 6. Typical plasma emission signal shape. Top line: emission signal at $Z_{\parallel} = 2.6$ mm. Bottom line: total emission signal.

opposite direction of the laser beam, $Z_{\parallel} \propto t_l^{0.65}$. After 200 ns from gas breakdown, the relation of Z_{\parallel} and t_l becomes $Z_{\parallel} \propto t_l^{0.38}$. The value of Z_{\perp} is related to the value of t_l by $Z_{\perp} \propto t_l^{0.5}$ in the vertical direction of the laser beam.

Figure 8 shows the change of the radiation jump time t_l of section $t_l - t_h$ in the position $Z_{\parallel} = 3$ mm with the laser energy E and pressure P . The result shows that, in

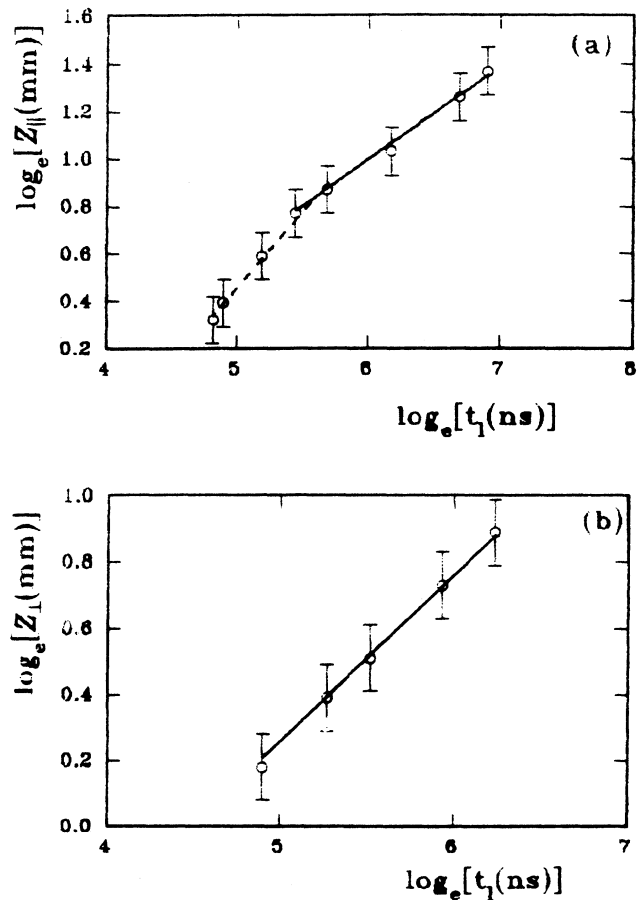


FIG. 7. (a) Distance Z_{\parallel} vs propagation time t_l . (b) Distance Z_{\perp} vs propagation time t_l .

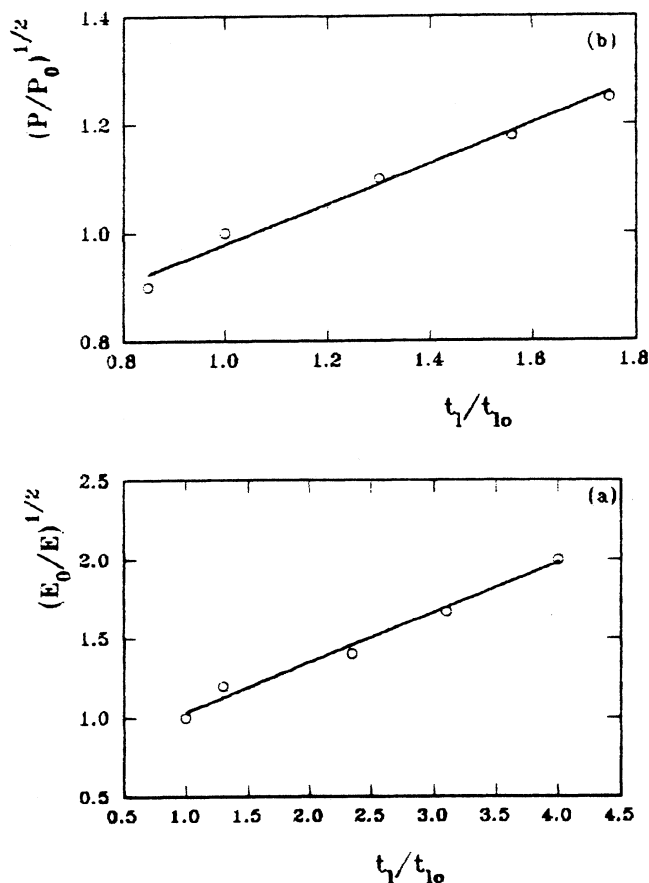


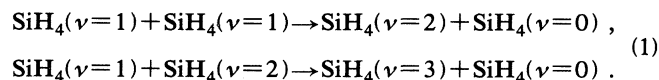
FIG. 8. (a) The relation of t_l and total pressure P at $Z_{\parallel}=3$ mm. t_{l0} corresponds to $P=200$ torr and $E=0.7$ J/pulse. (b) The relation of t_l and laser energy E at $Z_{\parallel}=3$ mm. t_{l0} corresponds to $P=200$ torr and $E=0.35$ J/pulse.

the same spatial position, the time of the expansive wave arrival is directly proportional to the square root of gas pressure P and inversely proportional to the square root of laser energy E .

IV. DISCUSSION

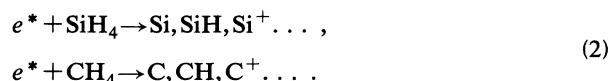
A. Breakdown processes in $\text{SiH}_4 + \text{CH}_4$ system irradiated by laser

For the interaction of $\text{SiH}_4 + \text{CH}_4$ with the CO_2 laser, since the wave number of the CO_2 10P(20) laser output is very close to that of an absorption transition in SiH_4 (ν_4 , 944.12 cm^{-1}), SiH_4 molecules will be excited to the first vibrational state by resonance absorption of a photon, and then by molecular collision, near resonance V - V energy transfer, such as



...

Some SiH_4 molecules will be excited to a higher quasicontinuum state. This photon absorption mainly occurs between the ground and first excited states of the molecule, so that the absorption is selective and depends on the frequency of the laser [7,8]. The SiH_4 molecule in the quasicontinuum state will be dissociated by collisions or further photon absorption, and at the same time some SiH_4 molecules may also be ionized. Therefore, this process can provide the first group of electrons for the occurrence of plasma. These electrons may obtain more energy in the intense laser field through the process of inverse bremsstrahlung, and cause the SiH_4 and CH_4 molecules to dissociate and ionize by collision, resulting in the formation of a plasma. This process could be described as



As the experimental results of OES, we obtain a larger number of characteristic emissions of H, Si, Si^+ , C, C^+ , etc. In this process the absorbed energy of electron is determined only by the laser intensity [9]. In our previous work [10], the breakdown of SiH_4 gas in the pressure range from 50 to 350 torr has been studied carefully. These results have shown a correlation of laser frequency to the breakdown of SiH_4 molecules, the identity of the frequency effect on the threshold value of SiH_4 molecule breakdown, and the linear absorption of SiH_4 molecules by the optoacoustic spectrum. In addition, for the same laser frequency, the intensity of the plasma radiation is proportional to the power of the incident laser. These results show that the formation of SiH_4 plasma depends strongly on the laser frequency. So we conclude that the breakdown process of the $\text{SiH}_4 + \text{CH}_4$ system in the CO_2 laser field is that of optical resonance absorption.

B. Electronic temperature and density of plasma

Since the molecular dissociation of SiH_4 and CH_4 in the laser-induced plasma will produce a large amount of Si, C, and H particles and various radicals containing Si, C, and H, collisions among dissociated fragments will bring about complex chemical reactions. The two principal parameters of the plasma—electron temperature and electron density—will directly affect the rate of these chemical reactions. Based on the theory of inverse bremsstrahlung, and assuming that during the heating processing of the laser the plasma absorbs all the laser energy for a short period of time t , the temperature of the plasma is [11]

$$KT_e = \frac{1}{6} W t^3 / (N_e + N_i), \quad (3)$$

where W is the power of the laser, N_e and N_i , respectively, are the number of electrons and ions in the breakdown area, and t is the heating time which is determined by $Kr=1$ (K is the absorption coefficient of inverse bremsstrahlung. In typical experimental conditions, the primary radius of the plasma is $r=0.1$ cm, equal to the radius of focal point of laser beam). The output power of the laser is $W=4.5 \times 10^6 \text{ W/cm}^2$, and the gas pressure is 200 torr, giving the time $t=46$ ns while the plasma tem-

perature is $T_e = 4.1$ eV.

Since, in our calculation, sample absorption of the laser energy before the breakdown of gases has been neglected, as well as other energy losses such as radiation of the plasma, gas expansion, etc., this calculated value is reasonably consistent with the experimental result $T_e = 3.6$ eV. In this temperature range, possible spectral broadening mechanisms of the dissociated fragments in the plasma include Doppler broadening, turbulence broadening, and Stark broadening. Turbulence broadening is determined by the thermal motion of the particles, and their linewidth is proportional to the central wavelength of the emission [12,13]. However, this conclusion is opposite to the experimental result. The FWHM value of the Doppler broadening is [14]

$$\Delta\lambda = 2\lambda_0[2kT(\ln 2)/M]^{1/2}/c, \quad (4)$$

where λ_0 is the center wavelength of the emission, k is Boltzmann's constant, and T and M , respectively, are the temperature and mass of the emitting particle. Within this temperature range, $\Delta\lambda$ of H β emission is about 0.1 nm, and this value is much less than the experimental result. So in our system, the broadening of the spectral line of the H atom must be due mainly to Stark broadening caused by the Coulomb field of charged particles in the Debye sphere of the radiating atoms. Hence, according to the approximate relationship of the width of the spectral line and the electronic density from [15],

$$\Delta\lambda = 2.18 \times 10^{-11} N^{2/3} \text{ (nm)}. \quad (5)$$

Taking note of the measured result of the time resolution of H β emission, we obtain the curve of the electronic density variation with time as Fig. 9. This result shows that, 100 ns after the laser pulse, the electron density in the focal area of the plasma is about $7 \times 10^{17} \text{ cm}^{-3}$, and then the density decreases with the time. The two quasistatic Stark components of H β emission caused by the ionic field will become more nearly equal with time, and the central dip of the H β emission will become shallower. Based on the experimental result, we find that the change of the inverse of the electronic density with time nearly satisfies a linear relation. This result shows that the main

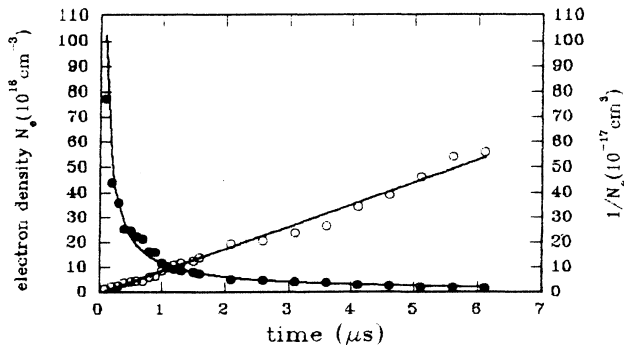


FIG. 9. The electron density vs time. ●, N_e (10^{16} cm^{-3}). ○, $1/N_e$ (10^{-17} cm^3).

process of neutralization in the plasma is the recombination of ions and electrons [6].

C. Fluid dynamic processes in laser-induced plasmas

After the formation of the plasma, in the area of breakdown, an instantaneous high temperature occurs and, around this area, there are fields of high gradient temperature and pressure. The plasma expands rapidly, and brings about a supersonic shock wave. The front of the plasma expansion wave is the front of the shock wave. The propagation of this shock wave heats the gases around it, and brings about ionization. Because of the absorption of the laser energy during a laser pulse, it makes the wave front propagate more rapidly in a direction opposite to the laser beam. This process is similar to that of a detonation wave in an explosive. In the vertical direction of a laser beam, and after the laser pulse, the propagation of the plasma wave is a supersonic and adiabatic expansion. In the direction opposite to the laser beam, during the time of a laser pulse and with the approximation of a plane wave, we obtain the relation of the plasma wave propagation velocity U in the focal area [9]:

$$U = [2(\gamma^2 - 1)P(t)f/\rho_0\pi Z^2 \tan^2\theta]^{1/3}. \quad (6)$$

In Eq. (6), $P(t)$ is the output power of the laser, θ is the convergence angle of the focused laser beam, which is constant; γ is the efficient adiabatic index depending on temperature and density; and f is the absorption coefficient of the laser energy. From Fig. 7, within a period of 200 ns, in the direction opposite to laser, we have $Z_{\parallel} \propto t^{0.65}$, which agrees with the integrated result of Eq. (6): $Z \propto t^{0.6}$, when the power of laser $P(t)$ is a constant. Thus the wave propagation in the direction opposite to the laser beam is more rapid than that in the vertical direction because of the absorption of laser energy. Therefore, the shape of the expansion of the plasma appears as an ellipsoid [16]. After the end of the laser pulse, the process of the plasma expansion satisfies a larger Mach's intense shock wave approximation,

$$Z = Y(\gamma)[W/\rho_0]t^\alpha, \quad (7)$$

where $Y(\gamma)$ is a constant depending on the adiabatic index, W is the laser energy absorbed by the plasma, and α is related to the shape of the wave (for a sphere, $\alpha = 2/5$). In the same spatial position, the arrival time of the shock wave is related to the laser energy E and pressure P . Along the direction of the laser beam, after $t = 200$ ns, the experimental result shows $Z_{\parallel} \propto t^{0.38}$. From Fig. 8, we see that the starting time t_l of the signal of the intense radiation in the direction opposite to the laser varies with the laser energy and the pressure, the result being

$$\frac{t_{l1}}{t_{l2}} \propto \left(\frac{P_1/P_2}{E_1/E_2} \right)^{1/2}. \quad (8)$$

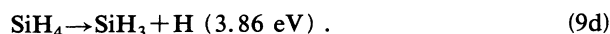
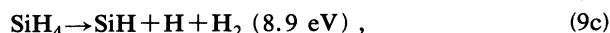
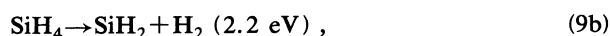
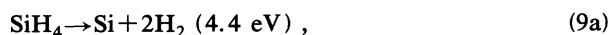
In the vertical directions of the laser beam, because of the ellipsoid shape of the primary plasma, the expansion of the plasma wave should be the same as the traveling of a cylindrical shock wave. This conclusion can be used to

explain the experimental result of $Z_{\perp} \propto t^{0.5}$. Hence the breakdown of $\text{SiH}_4 + \text{CH}_4$ produces an explosion resulting in the induction of a shock wave, and this process is the basic macrodynamic process in the plasma.

D. Dissociation kinetics of $\text{SiH}_4 + \text{CH}_4$ in laser-induced plasma

The action of the laser on the $\text{SiH}_4 + \text{CH}_4$ system brings about a plasma and causes the dissociation of SiH_4 and CH_4 . Hence determining the main dissociation process is important for the study of nanometer ceramic synthesis. At the time of the strongest action of the laser on the system, the radiation of the plasma is also most intense. From Fig. 4, we can see that the radiation reaches its maximum value at 50 ns, corresponding to the peak value of the laser pulse, and the temperature of the plasma is also a maximum. Obviously, at this time, the dissociation of SiH_4 and CH_4 is also the most intense, so that a large amount of first order dissociation fragments occur. Taking note of the characteristic of the dissociation in the plasma, the distribution of electron energy in the system is an important parameter for determining the primary dissociation channel of molecules.

For SiH_4 , possible dissociation channels and their dissociation energies are



The theory and experimental results show in detail that the process of $e\text{-SiH}_4$ scattering has a maximum cross section when the electron energy is 4.3 eV [17,18]. Noting that the average electron energy is 4.4 eV ($T = 3.6 \text{ eV}$) in this experiment, the dissociation of SiH_4 molecules will be mainly through channel (9a), producing Si atoms. For CH_4 , the dissociation channel: $\text{CH}_4 \rightarrow \text{C} + 2\text{H}_2$ needs an energy of about 8.3 eV. With electrons of 4.3-eV energy the collision process of $e\text{-CH}_4$ possesses a relatively large scattering cross section. If the energy distribution of electrons is nearly Maxwellian in the plasma, nearly 50% of the electrons possess an energy which is larger than that needed energy to produce C atoms from CH_4 molecules. Hence we consider that the rate of the dissociation of CH_4 into a C atom is relatively high. In addition, from the time characteristic of various emitting fragments in the plasma, we see that the radiation of Si, C, and H atoms possess different time characteristics from other atoms. The risetime of the emission of Si, C, and H is about 50 ns, corresponding to the time when the plasma possesses the highest temperature. Within a period of time after 50 ns [for Si(390.6 nm), ~ 150 ns; for H_{β} , ~ 150 ns, and for C (247.8 nm), ~ 500 ns], the emitting intensities increase slowly. This may be due to the collisions among reacting molecules and dissociated fragments, resulting in a further dissociation which produces additional C, Si, and H. These emitting fragments do not disap-

pear until 10 μs after the end of the laser pulse. The time of radiation is relatively short for other fragments, so that in the laser-induced plasma we see that the dissociation of SiH_4 and CH_4 depends mainly on the Si and C atom channels. With this conclusion, we can explain the experimental result of the time characteristic of plasma radiation.

1. Background character of the plasma radiation

The $\text{SiH}_4 + \text{CH}_4$ system is broken down by the laser, resulting in the occurrence of a plasma. Some dissociated fragments which are in excited states will emit their characteristic spectral radiation. Meanwhile, bremsstrahlung and transitions between bound and free states of radicals give a broad background radiation on the plasma OES. In Fig. 2, we see the background within our spectral range. No fragments possess characteristic emission at 625.0 nm. The time resolution measurement of the background radiation shows that the maximum value is reached at about 50 ns after the gas breakdown, then decreases quickly (see Fig. 4). Noting that the peak value of the laser pulse occurs near $t = 50$ ns, this is when the action of the laser on the gases is most intense, so that the plasma background is at a maximum. With the decrease of the laser intensity, along with the loss of energy by chemical reaction and collision and its expansion in the form of a shock wave, the energy in the plasma and the background radiation of the plasma decrease quickly.

2. Production and reaction of Si_2 , SiH , Si^{2+} , C^+ , and CH

As a result of the high temperature inside the plasma, collisions among particles are very frequent. The collision of dissociated fragments of SiH_4 and CH_4 will produce products such as



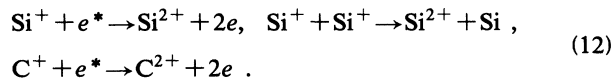
From the signals of the upper trace in Fig. 4, we see that a peak of plasma luminescence occurs 300–400 ns after breakdown. This luminescence peak is the emission of second order products. Since in our experiment the sample gases are SiH_4 and CH_4 , the occurrence of the Si_2 molecule is certainly related to the second order reaction; for example, the collisions among two Si atoms and the third particle M can produce the Si_2 molecule via equation (10a). In Fig. 4(c), we see that the emitting peak of Si_2 is about 300 ns, corresponding to the position of the second peak of the luminescence. Though the signal has a small peak at the rise time of 100 ns, its main contribution should be attributed to the influence of the plasma radiation background. Since the time characteristic of the emission of the SiH wavelength at 412.8 nm is similar to that of Si_2 , we believe that its occurrence is due mainly to second processing, i.e.,



For CH , because of its weak emission, the time charac-

teristic of the emission of CH is not observed. However, the experiment shows that the intensity dependence with reactant pressure of the emission of CH is similar to that of Si₂ and SiH [19], so we believe that it occurs from collision processes.

Si²⁺ (455.2 nm) and C⁺ (426.7 nm) occur at about 300 ns, and the spectral peak of C²⁺ (229.7 nm) appears at 400 ns. Therefore, we see that Si²⁺, C⁺, C²⁺, Si₂, and SiH are mainly second order products, for example



3. Occurrence and reaction of Si⁺ ion

The rise time of the Si⁺ emission signal at 634.7 nm is the same as the radiating characteristic of Si (288.1 nm). It has a relatively quick rise time (about 50 ns). Thus Si⁺ production should be of first order; that is,



The only difference is that the duration of the emission of the Si⁺ ion is short relative to that of the Si atom. This difference is partly due to ions combining with electrons, resulting in neutral particles with the decrease of plasma temperature; that is,



In addition, the occurrence of second order products depends mainly on the collision of particles in the system,

and their emitting intensities are closely related to the gas pressure. The experimental result has proved the above conclusion. The result about emitting intensities of first and second order products related to the gas pressure will be published in another paper [19].

V. CONCLUSION

The reaction of the low-temperature plasma includes complex physical-chemistry processes. In this paper, the optical emission spectrum with time and space resolution has been used to study the macrodynamic and microdynamic processes in the pulsed-laser-induced plasma of SiH₄+CH₄. The results obtained in our experiment have clearly given the properties of the plasma expansion, neutralization, and reaction processes of the dissociated fragments in the plasma. Based on the measurement of the time resolution of the emitting spectrum, the average electronic temperature and density of the plasma has also been obtained. Our work has provided important data for the study of dynamic processes in a low-temperature plasma, and the synthesis of a superfine powder of SiC by means of laser-induced plasma.

ACKNOWLEDGMENTS

The authors would like to thank Professor Xu Jiren and Professor Zhang Zhisan of the Institute of Physics, Chinese Academy of Science, for their exciting discussions, and Professor Jeffrey I. Steinfeld, Massachusetts Institute of Technology, for his helpful comments.

-
- [1] Fu Guangsheng, Han Li, Li Xiaowei, Zhang Lianshui, Dong Lifang, and Lu Furun, *Acta Phys. Sin.* **36**, 293 (1987).
 - [2] E. Borsela, L. Caneve, and A. Giardini, in *Laser Processing and Diagnostics (II)*, edited by D. Bäuerle, K. L. Kompa, and L. Laude (Les Editions de Physique, Les Ulis, 1986), p. 61.
 - [3] Han Li, Yu Wei, Fu Guangsheng, Li Xiaowei, and Zhang Lianshui, *Chin. J. Lasers A* **21**, 522 (1994).
 - [4] E. Borsela *et al.*, *Appl. Surf. Sci.* **36**, 213 (1989).
 - [5] H. P. Graf and T. K. Kuenbukl, *Appl. Phys. B* **31**, 53 (1983).
 - [6] Xing Xing, Wang Lixin, Huang Nantang, and Xu Jiren, *Chin. Phys. Lett.* **5**, 317 (1988).
 - [7] Dong Lifang, Fu Guangsheng, Li Xiaowei, Han Li, Zhang Lianshui, and Lu Furun, *Chin. J. Semicond.* **10**, 280 (1989).
 - [8] D. Touneau *et al.*, *Chem. Phys.* **103**, 353 (1986).
 - [9] T. P. Hughes, *Plasma and Laser Light* (Hilger, London, 1975), p. 145.
 - [10] Zhang Lianshui, Zhang Guiyin, Fu Guangsheng, Han Li, and Zhang Kaixi, *Chin. J. Lasers A* **19**, 624 (1992).
 - [11] J. Dawson, *Phys. Fluids* **7**, 981 (1963).
 - [12] E. J. Iglesias and H. R. Griem, *Phys. Rev. A* **38**, 301 (1988).
 - [13] J. Wang and H. R. Griem, *Phys. Rev. A* **40**, 4115 (1989).
 - [14] A. Corney, *Atomic and Laser Spectroscopy* (Clarendon, Oxford, 1977), p. 236.
 - [15] V. Helbig and K. P. Nick, *J. Phys. B* **14**, 3573 (1981).
 - [16] R. M. Armstrong, C. S. Coffey, V. F. DesVost, and W. L. Elban, *J. Appl. Phys.* **63**, 979 (1990).
 - [17] A. K. Jain, A. N. Tripathi, and A. Jain, *J. Phys. B* **20**, L389 (1987).
 - [18] Yuan Jianmin, *Chin. J. At. Mol. Phys.* **7**, 1399 (1990).
 - [19] Han Li *et al.*, *Spectrosc. Spectral Anal.* **15**, 65 (1995).